

PDF hosted at the Radboud Repository of the Radboud University Nijmegen

The following full text is a publisher's version.

For additional information about this publication click this link.

<http://hdl.handle.net/2066/98969>

Please be advised that this information was generated on 2019-05-21 and may be subject to change.

Excitation of C₆₀ using a chirped free electron laser

Gert von Helden, Iwan Holleman, and Gerard Meijer

*Dept. of Molecular and Laser Physics, University of Nijmegen
Toernooiveld, NL-6525 ED Nijmegen, The Netherlands*

*and
FOM-Institute for Plasma Physics Rijnhuizen
Edisonbaan 14, NL-3430 BE Nieuwegein, The Netherlands*

gertvh@sci.kun.nl

Boris Sartakov

*General Physics Institute, Russian Academy of Sciences
Vavilov str. 38, 117942 Moscow, Russia*

Abstract: Gas phase C₆₀ is resonantly excited using picosecond infrared (IR) pulses from a free electron laser. The excitation can be very high, reaching levels where the thermal emission of electrons from C₆₀ is observed. The excitation is much more efficient when the IR radiation is chirped to lower frequencies during the excitation process. The excitation process is modeled and the results are compared to the experiment.

©1998 Optical Society of America

OCIS codes: (020.0020) Atomic and molecular physics;(300.6410) Spectroscopy, multiphoton

References and links

1. T. Leisner, K. Athanassenas, O. Echt, O. Kandler, D. Kreisler, and E. Recknagel, "Hot tungsten clusters - competition between atom ejection and thermionic emission," *Z. Physik D* **20**, 127 (1991).
2. A. Amrein, R. Simpson, and P. Hackett, "Delayed ionization following photoexcitation of small clusters of refractory elements - nanofilaments," *J. Chem. Phys.* **94**, 4663 (1991).
3. E.E.B. Campbell, G. Ulmer, and I.V. Hertel, "Delayed ionization of C₆₀ and C₇₀," *Phys. Rev. Lett.* **67**, 1986 (1991).
4. P. Wurz and K.R. Lykke, "Delayed electron emission from photoexcited C₆₀," *J. Chem. Phys.* **95**, 7008 (1991).
5. D. Ding, J. Huang, R.N. Compton, C.E. Klotz, and R.E. Haufler, "Cw laser ionization of C₆₀ and C₇₀," *Phys. Rev. Lett.* **73**, 1084 (1994).
6. M. Hippler, M. Quack, R. Schwarz, G. Seyfang, S. Matt, T. Märk, "Infrared multiphoton excitation, dissociation and ionization of C₆₀," *Chem. Phys. Lett.* **278**, 111 (1997).
7. G. von Helden, I. Holleman, G.M.H. Knippels, A.F.G. van der Meer, and G. Meijer, "Infrared resonance enhanced multi photon ionization of fullerenes," *Phys. Rev. Lett.* **79**, 5234 (1997).
8. G. von Helden, I. Holleman, A.J.A. van Roij, G.M.H. Knippels, A.F.G. van der Meer, and G. Meijer, "Shedding new light on thermionic electron emission of fullerenes," *Phys. Rev. Lett.* **81**, 1825 (1998);
<http://mlfsilly.sci.kun.nl/~denizvh/IRREMPI.html>
9. D. Oepts, A.F.G. van der Meer, and P.W. van Amersfoort, "The free-electron-laser user facility FELIX," *Infrared Phys. Technol.* **36**, 297 (1995);
<http://www.rijnh.nl/DEPARTMENTS/LASER/FELIX/felix.html>
10. G.M.H. Knippels, A.F.G. van der Meer, R.F.X.A.M. Mols, D. Oepts, P.W. van Amersfoort, A.M. MacLeod, and W.A. Gillespie, "Feasibility of a far-infrared free-electron laser as a voltage-controlled oscillator," *Infrared Phys. Technol.* **37**, 285 (1996).
11. D.S. Bethune, G. Meijer, W.C. Tang, H.J. Rosen, W.G. Golden, H. Seki, Ch.A. Brown, and M.S. de Vries, "Vibrational raman and infrared spectra of chromatographically separated C₆₀ and C₇₀ fullerene clusters," *Chem. Phys. Lett.* **179**, 181 (1991).
12. V.N. Bagratashvili, V.S. Letokhov, A.A. Makarov, and E.A. Ryabov, *Multiple Photon Infrared Laser Photophysics and Photochemistry*, Harwood Academic Publishers (1985).

13. L. Nemes, R.S. Ram, P.F. Bernath, F.A. Tinker, M.C. Zumwalt, L.D. Lamb, and D.R. Huffman, "Gas-phase infrared emission spectra of C₆₀ and C₇₀ - temperature-dependent studies," Chem. Phys. Lett. **218**, 295 (1994).
 14. C.E. Klots, R.N. Compton, "Evidence for thermionic emission from small aggregates," Surf. Rev. Lett. **3**, 535 (1996).
-

Introduction

Fullerenes and metal clusters have been the first neutral molecules for which thermionic emission of electrons, the microscopic equivalent of the electron emission from heated surfaces, has been observed. In these experiments [1,2,3,4] the excitation is done using wavelengths ranging from the UV to the near-IR. In these cases, the initial photon absorption occurs on electronic transitions which are assumed to relax fast to highly vibrationally excited levels in the electronic ground state. After absorption of several photons, the internal energy can be high enough (30–50 eV) such that thermionic electron emission takes place. Further support for such a mechanism stems from experiments where C₆₀ is being ionized using a cw argon ion laser [5].

More direct insight in the processes involved can be obtained when the vibrational modes of fullerenes are excited directly, by using fixed frequency [6] or tunable IR radiation [7,8]. When being resonant with an IR active mode, efficient ionization of the fullerenes is observed and ionic fragmentation products, such as C₅₈⁺ and C₅₆⁺, are almost completely absent. By tuning the wavelength of the excitation laser, distinct resonances are observed and lines in the resulting IR resonance enhanced multiphoton ionization (IR-REMPI) spectrum are all observed to be red shifted, compared to the linear absorption IR spectrum of solid C₆₀ at room temperature. The excitation process is thought to be sequential single photon absorption followed by internal vibrational redistribution (IVR). After absorbing several hundred photons, the internal energy in the molecules has build up to levels where thermionic electron emission can occur.

In this IR multiple photon excitation scheme, the IR active vibrations are anticipated to stay resonant with the excitation laser up to rather high internal energies, since, with 174 degrees of freedom, the number of quanta excited per mode is still moderate. The shift of a resonance is therefore expected to be determined by comparatively weak cross-anharmonicities rather than by the stronger regular anharmonicity of the IR active mode. As a consequence, one might expect that the intrinsic width of a resonance at a given time in the excitation process can be rather narrow, with the position of this line shifting in time. The observed shape of the lines in the IR-REMPI spectrum is then governed by the range of resonance positions, starting from the resonance position of the molecules coming from the source to that of molecules that have a sufficient energy for efficient autoionization. In such a scenario, frequency chirping of the excitation laser might dramatically enhance the overall excitation efficiency. In this paper, the IR excitation mechanism of C₆₀ is studied both experimentally and theoretically and the various conjectures described above are tested.

Experimental

The experimental setup has been described previously [7,8] and is shown in Fig. 1. A beam of C₆₀ is generated by heating C₆₀ in a quartz oven to 700–850 K. The effusive beam is intersected by the IR laser beam between the plates of a Time-Of-Flight (TOF) mass spectrometer. The IR laser enters the apparatus several cm above, and co-propagating with, the fullerene beam. A spherical mirror with a focal length of 7.5 cm focuses the IR light on the fullerene beam. A second mirror, again at a distance of 7.5 cm from the focus, acts as a retroreflector and focuses the IR beam such that both foci overlap, resulting in a doubling of the micropulse repetition rate in the focus (*vide infra*). The optical cavity is inclined with respect to the molecular beam to increase the

interaction time of the molecules with the focused IR light. The residence time of the molecules in the laser focus is estimated to be several μs . The TOF consists of three stainless steel plates that are 1.5 cm apart. Ions are detected on a multi channel plate (MCP) detector at a distance of 45 cm from the last TOF plate. The first two TOF plates are pulsed from ground to high voltage (5 kV and 4 kV), typically 30 μs after the IR laser pulse. Ions are detected on a MCP detector and the signal is recorded on a digital oscilloscope. IR-REMPI spectra are recorded by measuring the C_{60}^+ signal intensity as a function of IR laser wavelength.

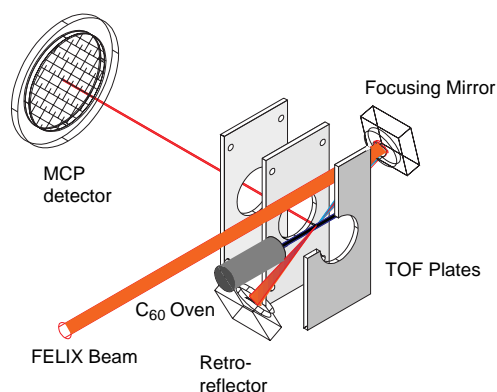


Fig. 1. Schematic of the experimental setup.

Experiments are performed at the ‘Free Electron Laser for Infrared eXperiments’ (FELIX) user facility in Nieuwegein, The Netherlands [9]. FELIX produces IR radiation that is continuously tunable over the $40\text{--}2000\text{ cm}^{-1}$ range. The light output consists of macropulses at 10 Hz of about 5 μs duration containing up to 100 mJ of energy. A macropulse consists of a train of micropulses with a typical (adjustable) duration of 0.3–5 ps that are 1 ns apart. The attainable bandwidth is near Fourier-transform limited, and is varied between 2 and 0.4 % of the central frequency for the experiments described here. By putting a ramp on the electron beam energy of the laser, its wavelength can be chirped either up or down during the macropulse. The maximum amount of chirp attainable is limited by the electron beam optics of FELIX and by the gain characteristics of the free electron laser to a few percent of the laser wavelength [10].

Results

In Fig. 2, the C_{60} ion intensity as function of the IR laser frequency, the IR-REMPI spectrum, is shown. The IR-REMPI spectrum is very similar to the one shown previously [7], and the four strongest resonances correspond to the four well-known IR allowed transitions of C_{60} [11]. Relative to the IR absorption spectrum of solid C_{60} all lines in the IR-REMPI spectrum are red shifted, with the lines exhibiting the least red shift appearing most intense in the IR-REMPI spectrum. The observation of ionization after IR excitation might be unexpected since it requires very many photons to be absorbed. To observe, for example, ion signal at a frequency of 520 cm^{-1} , an estimated 500–800 photons need to be absorbed by a single molecule. The purpose of this study is to investigate the excitation process in more detail and for this we will concentrate on the strong 520 cm^{-1} resonance, shown in red in Fig. 2.

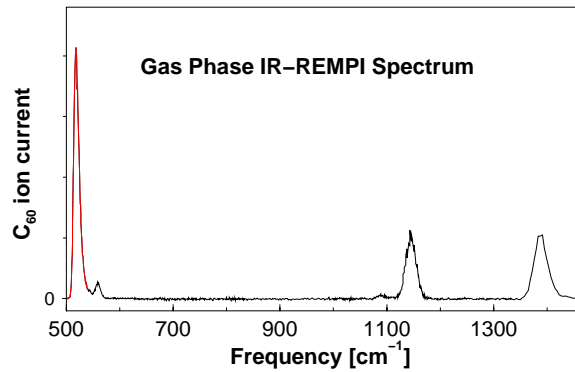


Fig. 2. IR-REMPI spectrum of gas-phase C_{60} .

While the resonance at 520 cm^{-1} is somewhat broad in Fig. 2, it is also observable with a reduced bandwidth of the excitation laser. In the lower trace of Fig. 3 this same peak is shown with a FWHM bandwidth of the excitation laser of about 2 cm^{-1} . The resulting IR-REMPI peak is surprisingly narrow, having a full width at half maximum of only 6.3 cm^{-1} . The peak is clearly asymmetric, having a tail towards higher frequencies, i.e., towards the position of the IR absorption line in room temperature solid C_{60} . In the upper trace of Fig. 3, the same peak is shown when a frequency chirped excitation laser is used. The wavelength scale is chosen such that it reflects the laser frequency near the start of the macropulse (see Fig. 4). When a frequency chirp is applied as indicated in the contour-plot shown in Fig. 4, a C_{60} ion signal increase of about a factor of thirty is observed relative to the situation without a frequency chirp. In addition, the resonance gets even narrower. The peak is still clearly asymmetric, tailing towards high frequencies. When frequency chirping towards higher frequencies is applied, no ion signal is observed.

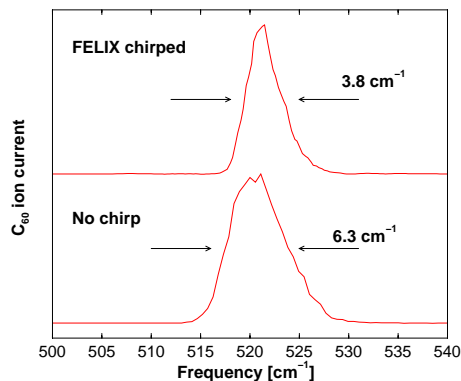


Fig. 3. IR-REMPI peak of gas-phase C_{60} recorded using a chirped (upper trace) and a non chirped (lower trace) excitation laser.

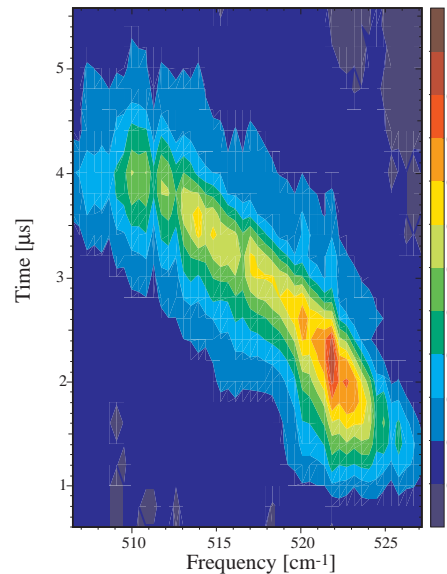


Fig. 4. False-color representation of the frequency of the excitation laser during the chirped macropulse. The wavelength setting of FELIX corresponds to the one used on the peak of the resonance shown in the upper trace of Fig. 3.

Theoretical Modeling

Being a large molecule, the mean internal energy of C₆₀ effusing from the oven at 800 K is with 39000 cm⁻¹ rather high, but with a whopping 10⁴⁸ states/cm⁻¹ at this internal energy, the density of states is even more remarkable. The density of states rapidly climbs to much larger values at higher energies, and the coupling between these many states due to vibrational anharmonicities results in very fast IVR. It is therefore safe to assume that the IVR process is much faster than the rate of photon absorption. The vibrational energy is then at any time statistically distributed over the vibrational degrees of freedom and the excitation process can be described using a statistical approach [6,12]. It is also expected that, due to the high density of states and the coupling between them, coherent excitation effects, such as chirped induced adiabatic passage, are not important in the experiments described here.

The individual levels in the ladder of levels that are in resonance with the excitation laser field are enumerated by the index $i = 0 \dots \infty$ and their energy E_i can be expressed as $E_i = \hbar\omega \cdot i$ where ω is the angular frequency of the laser radiation. The dynamics of the population distribution can be described by the kinetic equations

$$dn_i/dt = F_{i+1,i} + F_{i-1,i} - F_{i,i+1} - F_{i,i-1} \quad (1)$$

where n_i is the population of the i -th level and $F_{i,j}$ is the rate of the population flow between level i and j induced by the laser. $F_{i,j}$ can be written as

$$F_{i,j} = \frac{I}{\hbar\omega} \sigma_{i,j} \cdot n_i \quad (2)$$

where I is the laser intensity and $\sigma_{i,j}$ is the absorption cross-section of the $i \rightarrow j$ transition. The spectrally integrated absorption cross-section $A_{i,j}$ is defined by

$$A_{i,j} = \int \sigma_{i,j}(\omega) \cdot d\omega = 4\pi^2 \omega_{res} \cdot d_{i,j}^2 / \hbar c \quad (3)$$

where $d_{i,j}$ is the dipole moment matrix element of the transition and ω_{res} is the frequency of the molecular resonance. We assume that transitions in the ladder of levels are characterized by the statistically averaged values $\langle d_{i,j}^2 \rangle$ of the appropriate matrix elements. The relation between up and down transitions must satisfy the principle of detailed balance

$$\sigma_{i,i+1} / \sigma_{i+1,i} = A_{i,i+1} / A_{i+1,i} = g_{i+1} / g_i \quad (4)$$

with g_i the density of states at level i . The absorption cross-section of a vibrational band is given by

$$\sigma_{i,j}(\omega) = A_{i,j} \cdot f(\omega - \omega_{res}) \quad (5)$$

where $f(\omega - \omega_{res})$ is a normalized Lorentzian lineshape function, in which broadening of the line due to IVR and shifts of the resonant frequency due to anharmonicities are incorporated. The rotational contribution is neglected in view of the small rotational constant of C₆₀. We assume that both the width of the Lorentzian (FWHM), $\Gamma(E_i)$, and the resonant frequency depend linearly on the internal energy E_i as $\Gamma(E_i) = a \cdot i$ and $\omega_{res} = \omega_0 + b \cdot i$. The expression for $\sigma_{i,j}(\omega)$ has to be convoluted with the spectral profile of the excitation radiation, which is assumed to be a Lorentzian as well.

The parameters a and b are estimated from temperature dependent emission studies on gas-phase C₆₀ [13] as $a = 0.0165$ cm⁻¹ per quantum and $b = -0.017$ cm⁻¹ per quantum for the IR active mode with $\omega_0 = 527$ cm⁻¹. The spectrally integrated

absorption cross-section of this mode is obtained from FTIR data of solid C_{60} as $2.8 \cdot 10^{-17}$ cm.

In the calculations, an initial thermal distribution of populations is taken. The laser pulse is taken as a block-function in time with the same time-integrated fluence as used in the experiment. The set of differential equations (1) is solved numerically using the Runge-Kutta-Merson algorithm.

Discussion

Even without solving the differential equations, some features of the experimentally observed line-shape can be qualitatively understood by looking at the changes in the absorption profile with increasing internal energy. In Fig. 5 the IR absorption profile of C_{60} when it leaves the oven (blue trace; 800 K) is shown together with the absorption profile at high internal energies (solid red trace; 3000 K), energies at which autoionization is thought to become efficient.

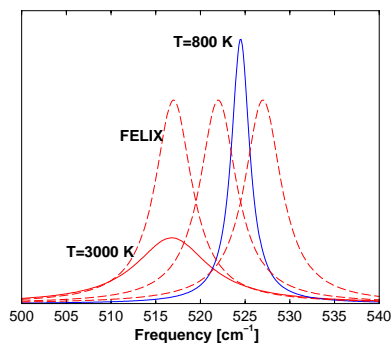


Fig. 5. IR absorption profiles of C_{60} at different internal energies (solid lines) together with three spectral profiles of FELIX (dashed curves).

When FELIX is being scanned from high to low frequency, it first has reasonable overlap with cold C_{60} but less ideal overlap with hot C_{60} . The molecules can thus not be excited high enough and a low ion signal is expected. When FELIX is moved towards lower frequencies, slowly overlap is gained with hot molecules while still being sufficiently resonant with cold C_{60} . The excitation and ionization efficiency will thus slowly be increased. With FELIX at still lower frequencies, while the overlap with hot molecules is further improved, the overlap with cold molecules is lost very fast. These qualitative arguments are consistent with the, initially maybe counterintuitive, peak shape observed in Fig. 3 in which a sharp rise at low frequencies and a longer tail at higher frequencies is observed.

In Fig. 6, the most probable excitation energy in the ensemble of molecules at the end of the FELIX pulse is shown as a function of excitation laser frequency. In the calculation, a laser fluence of 5 J/cm^2 and a laser bandwidth of 2.5 cm^{-1} is assumed. Both results for a non-chirped and a chirped (total frequency chirp -6.0 cm^{-1}) excitation pulse are given. The elevated baseline corresponds to the initial 800 K thermal energy of C_{60} .

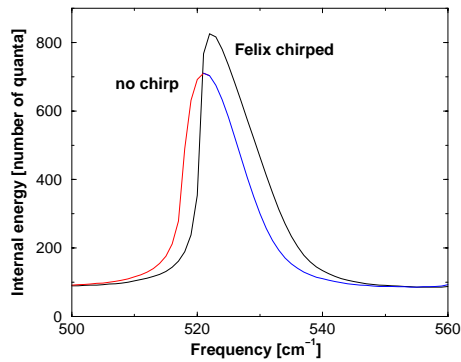


Fig. 6. Most probable excitation as a function of FELIX frequency. Shown is a simulation for a frequency chirped and a non chirped excitation laser.

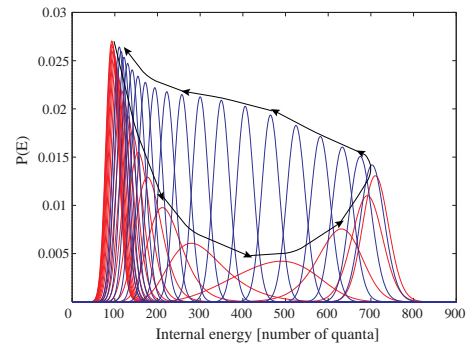


Fig. 7. Normalized internal energy distribution while scanning the non chirped FELIX pulse over the excitation line.

In Fig. 7, the normalized internal energy distributions are plotted for a series of frequencies (1 cm^{-1} apart) while scanning the unchirped excitation laser pulse from 500 to 540 cm^{-1} . The direction of increasing frequencies is indicated in the figure by arrows. While rather broad at the sharply increasing red side of the line, the distributions become much narrower at the blue side of the peak. The calculated excitation line profiles shown in Fig. 6 show resemblance with the corresponding line profiles observed in the IR-REMPI spectrum (Fig. 3). First, the peak position of $\approx 520 \text{ cm}^{-1}$ agrees rather well with the observed peak positions in the IR-REMPI spectra. Second, both for chirped and non-chirped excitation tailing of the line profile towards higher frequencies is observed as in the experiment.

The calculations clearly indicate that under the experimental conditions employed here, a single C_{60} molecule can indeed absorb more than 600 photons. The calculations also predict that chirping FELIX to lower frequencies results in an improved excitation efficiency. At first sight, this increase might not appear to be too dramatic. However, in Fig. 6 only the amount of excitation is plotted and not the ion yield. It is expected that the ion yield depends highly nonlinearly on the amount of internal excitation [14]. A small increase in excitation efficiency will therefore give rise to a large increase in ion yield, bringing the calculations in qualitative agreement with the experimental observations.

This work is part of the research program of the FOM, which is financially supported by the 'Nederlandse Organisatie voor Wetenschappelijk Onderzoek (NWO)', and receives direct support by the NWO via PIONIER-grant # 030-66-089. This work is also receives partial support by the EU (HCM network ERB-CHR-XCT-94-0603).